Aerospace Science and Technology 81 (2018) 225–236

Contents lists available at ScienceDirect

Aerospace Science and Technology

www.elsevier.com/locate/aescte

Numerical investigations on lifting and flow performance of finger seal with grooved pad

Xingyun Jia, Qun Zheng, Zhitao Tian, Yuting Jiang, Hai Zhang *

College of Power and Energy Engineering, Harbin Engineering University, Harbin 150001, China

ARTICLE INFO

Article history:
Received 21 March 2018
Received in revised form 1 August 2018
Accepted 8 August 2018
Available online 14 August 2018

Keywords:
Clearance control
Deformation
Finger seal
Fluid-structure interaction
Groove

ABSTRACT

We investigate non-contact finger seal owing to its potential to reduce the specific fuel consumption of a gas turbine engine by 2–3%. The compliance features combined with the non-contact characteristic permits the position adjustment of the finger seal to the rotor excursions without destroying the stability of the rotor-seal system. The grooved structures on the lift pad of the three-layer finger seal are proposed with a view to improve the lifting and leakage capacities. Two-way fluid-structure interaction (FSI) methods are used, and the results show that the grooved structures positively affect the sealing performance. First, an uneven clearance occurs because of the seal deformation. Next, the sealing flow field is changed owing to the grooved structure. Finally, the grooved structure is proven to improve the seal's lifting capability, and the vortices in the grooves improve the sealing performance. The vortices in the groove cavities contribute significantly to the improvement in the lifting and leakage capacities. The grooved structure changes the pressure distribution under the lift pad, and a larger force is generated on the bottom surface of the lifting pad.

1. Introduction

Rotor seals are an important part of the modern gas turbine engine. They have prominent effects on improving the aerodynamic performance of gas turbines [1]. Nevertheless, the progress of advanced gas turbines, in terms of their rotate speed and operating temperature, means that simple structural improvements of the rigid seal, such as labyrinth seal or honeycomb seal, can hardly solve the problems arising from excessive rotor vibrations, such as the rub-impact. In subsized turbines, the abrasion between the rotor and seal is more remarkable because it produces a much higher proportion of gas leakage compared with larger sized engines with similar amounts of abrasion. The use of a compliant seal, known as a finger seal, can improve this condition [2].

Hendricks [3] reported the initial numerical analysis of a finger seal, using a bulk flow model similar to that researched by Braun et al. [4,5] for a brush seal. Arora et al. [6] tested a pressure-balanced finger seal, and Proctor et al. [7] tested the application of a herringbone-grooved rotor on a finger seal, and acquired the wear and lifting characteristics of the tested seal. The fluid-structure interaction (FSI) method [8–11] was applied to a finger seal to capture the interaction between the finger seal and the fluid field. Braun [12,13] investigated the three-dimensional deformation using different configurations of a single padded finger and a double high pressure (HP)/single low pressure (LP) finger combination to determine the padded finger seal's structural response to an external pressure motivation. Braun analyzed the deformation using the one-way FSI method, which could yield the flow and steady-structure data; however, they did not provide the simultaneous real-time results.

The two-way FSI technique has been used to analyze the aerodynamic and deformation properties. Using the two-way FSI can overcome the weakness of the one-way FSI by facilitating the simultaneous analysis of the flow and structure. Thus, numerical simulations can be used analyze the real-time interactions between both fields. The authors used the two-way FSI technique to analyze finger seals in a previous work [14], and obtained data for the flow and structure.

The authors [14] have obtained the flow, leakage, and deformation characteristics of the generic finger seal configuration, as well as the hysteresis characteristics of the boots' lift. The authors have indicated that the lack of the finger seal boot height and the hysteresis of the lifting were caused by the insufficient aerodynamic force of the sealing flow field. Therefore, in this work, the authors propose to use the grooved structure on the bottom of the finger seal lift pad to enhance the lift performance. In addition, the effect of width and depth of the grooved structures on the lifting

* Corresponding author.
E-mail address: zhanghai83821@163.com (H. Zhang).

https://doi.org/10.1016/j.ast.2018.08.014
1270-9638/

Nomenclature

c	absolute velocity ..... m/s	Re	Reynolds number ..... –
D	deformation ..... mm		
ΔD	increment of deformation ..... mm	Abbreviations	
$\dot{m}$	mass flow rate ..... kg/s	CFD	Computational fluid dynamics
P	pressure ..... Pa	FSI	Fluid-structure interaction
r	radius ..... m	HP	High pressure
u	circumferential velocity ..... m/s	LP	Low pressure

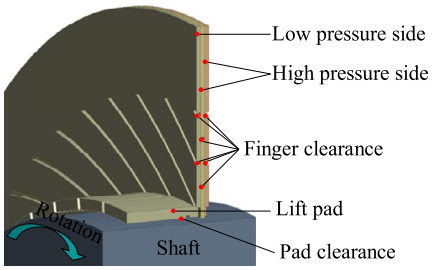

Fig. 1. Structure diagram of finger seal.

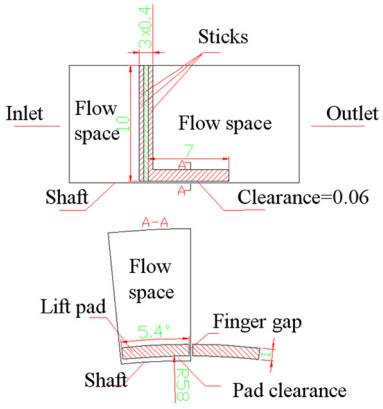

Fig. 2. Primary dimensions of finger seal.

and leakage capacities are compared from the perspective of vortex analysis in the grooved structure.

2. Model definition and validation

2.1. Geometry

Fig. 1 shows that the simulation geometry comprising three seal plates. In the typical structure of a finger seal, a HP zone exists with two rows of plates and no pad, and an LP zone with one row of padded finger plate that combines the strong rotational flow with the clearance between the pad and the rotor. Two leakage paths occur in the finger seal: the first is the pad clearance between the bottom surface of the lifting pad and the rotor, and the second is the finger clearance between the two finger elements. Figs. 2 and 3 display the detailed dimensions of the finger seal geometry, in which all the dimensions are in millimeters. The grooved structures are shown in Fig. 3. Three groove widths are shown in the computational model: 1.2 mm, 2 mm, and 3.2 mm. Two groove depths (0.3 and 0.2 mm) are investigated in this work.

2.2. Computational modeling and meshing

The visual FSI interfaces are displayed in Fig. 4 (a). In Fig. 4 (a), the object represents the solid domain, whereas the semitranspar-

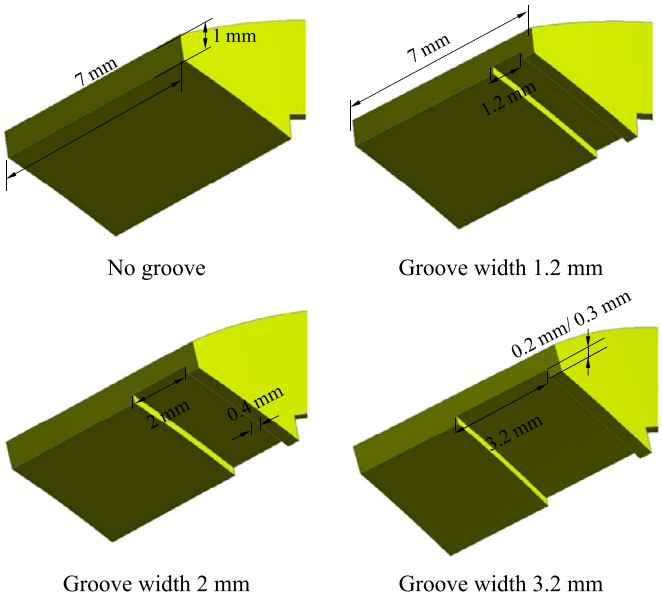

Fig. 3. Grooved structure used in the analysis.

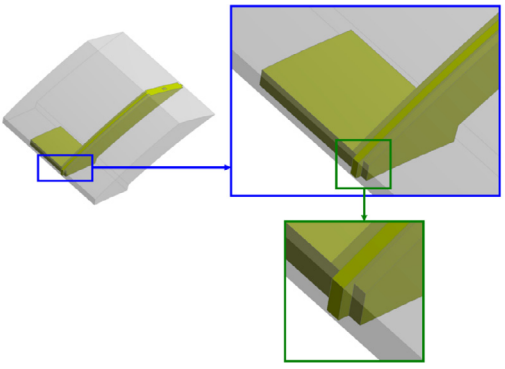

(a) Computational model of FSI

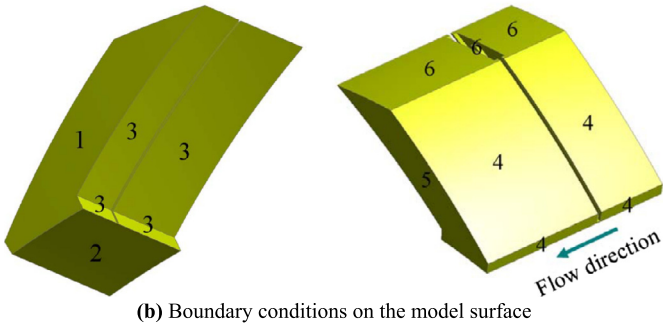

(b) Boundary conditions on the model surface

Fig. 4. Computational model of FSI and boundary conditions, (a) Computational model of FSI, (b) Boundary conditions on the model surface.